Вісник Тернопільського національного технічного університету
https://doi.org/10.33108/visnyk_tntu
Scientific Journal of the Ternopil National Technical University
2023, № 2 (110) https://doi.org/10.33108/visnyk_tntu2023.02
*ISSN 2522-4433. Web: **visnyk.tntu.edu.ua***

UDC 620.1:62-226.2

ESTABLISHING THE CAUSES OF PREMATURE DAMAGE OF STEAM TURBINE ROTOR BLADES OF TPP

Petro Solovei[1]; Oleksandra Student[1]; Lesia Svirska[1]; Ivan Kurnat[1]; Sofiia Krechkovska[2]; Taras Gural[1]

[1]Karpenko Physico-Mechanical Institute of the National Academy of Sciences of Ukraine, Lviv, Ukraine
[2]Lviv Polytechnic National University, Lviv, Ukraine

Summary. *The technical condition of the metal of the steam turbine blade was analyzed and the reasons for its fracture were established. It was shown that the relative elongation δ of the blade metal varied from 7.4 to 11.5%, and was lower than the regulated level. The low values of δ and the obtained values of the ratio between yield strength and ultimate tensile strength σ_{YS} / σ_{UTS}, which varied from 0.8 to 0.89, indicate a low margin of plasticity of the blade metal, which contributed to its cracking under the action of working loads. Metallographic analysis revealed pores in the surface-hardened layer of the blade. They caused low adhesion of the layer with the base metal of the blade, and also of crack initiation. The high stress concentration and the contact of the blade metal with the working medium contributed to the growth of a subcritical corrosion-fatigue crack in the cross-section up to its complete destruction.*

Key words: *15Kh11MF steel, steam turbine blade, strength, plasticity, impact toughness, structure*.

https://doi.org/10.33108/visnyk_tntu2023.02.046 *Received 02.03.2023*

Formulation of the problem. The rotor of a steam turbine is classified as a dangerous element because its destruction causes not only economic losses, but also threatens thermal power plant (TPP) personnel and the environment as well. The costs for the manufacture of the blades are 17...27% of the total cost of the entire turbine, and the complete blading is from 10...12%. Steam turbine blades are considered to be heavily loaded elements, so they are subject to mandatory technological control. Destruction of the blades in the initial stages of operation does not occur often, mainly due to violations of the manufacturing and installation technology, and also non-compliance with the regulated operating parameters of the turbines.

Among the frequent causes of blade damage are initiation and propagation of fatigue cracks from technological stress concentrators due to an excessively high level of vibration and, accordingly, an increase in the amplitude of cyclic loads with a high static component of the load, caused by the impact of excessive centrifugal forces on the blades, which ensures a high asymmetry of their load cycle. Besides, during the blades operation, additional influences cannot be avoided, in particular bending and torque moments, working high-temperature and corrosive-active environment, which brings to erosion, cavitation, facilitates the propagation of corrosion-fatigue cracks, etc. Such destruction of even individual blades of any stage of the rotor can cause failure of the entire turbine if it is not stopped in time.

In general, the performance of the elements of the blade apparatus of a steam turbine depends on the structure of heat-resistant steel, their mechanical properties [1–11], fatigue characteristics, static and cyclic crack resistance [12–17], the embrittlement effect of the technological environment [18–21] and the degradation of steel at the microstructural level during long-term operation [15, 22–25]. It is clear that in the initial state, the mechanical characteristics and structure of the steel must correspond the requirements stipulated by the

 Corresponding author: Lesia Svirska; e-mail: lesyasvirska@gmail.com

current regulatory documents. If this condition is met, it is important to ensure the stability of these properties during operation. Actually, this is a guarantee of the integrity of the rotor elements during long-term operation. Given the extreme importance of the reliability of the blade apparatus and the danger of consequences from their damage, one of the important tasks is to analyze the reasons of their damage in order to take into account the experience gained during the operation of other turbines and the design of new units.

Objectives of the research. Based on the assessment of the mechanical properties of strength, plasticity and impact toughness of the metal, hardness measurements and metallographic studies of the metal structure, find out the causes of damage to the steam turbine blade.

Object and methods of the research. A fragment of the working blade of the low-pressure cylinder of the TPP turbogenerator after 7400 h. of operation and 8 shutdowns of the technological process (Fig. 1) was studied. The blade is made of 15Kh11MF steel. The content of chemical elements in it did not exceed the limits regulated for this steel (Table 1).

Table 1

Chemical composition of the blade metal, wt. %

C	Si	Mn	Cr	S	P	Ni	V	Mo	Cu	Fe
0.17	0.30	0.45	10.50	0.0035	0.0005	0.20	0.34	0.73	0.08	Balance
Regulated content of the elements (RD 153-34.1-17.462-00)										
0.12…0.19	0.50	0.70	10…11.5	0.025	0.03	0.60	0.25…0.40	0.6…0.80	0.30	Balance

The technical condition of the blade metal was assessed by standard tensile mechanical characteristics. The characteristics of strength (ultimate tensile strength σ_{UTS} and yield strength σ_{YS}) and plasticity (elongation δ and Reduction of area ψ) were determined on smooth cylindrical specimens with a diameter of 5 mm and five times the length of the working part. Specimens were made from the peripheral (deformed) part of the feather of the blade, its about-shank part, and from the shank. In order to eliminate grinding marks, which could serve as stress concentrators during tensile tests, the samples were polished with polishing pastes of different grain sizes. According to the recommendations [26], the samples were loaded in tension until failure on the UME-10T machine.

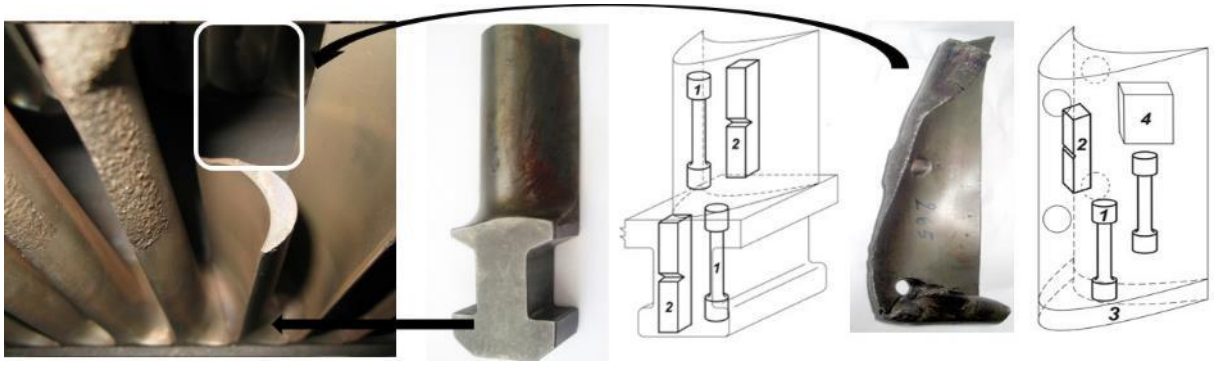

Figure 1. Macro view of broken blade and the scheme cutting of specimens for tensile (1) and impact (2) testing, the chemical composition estimation (3) and metallographic analysis (4)

In addition, the technical condition of the blade metal was also estimated by the impact toughness, which was determined on the Charpy V-notch specimens with a tip *radius* of

0.25 mm and *Mesnager* U-notch specimens with a tip *radius* of *1 mm*. During the tests, the requirements [27] were followed. The scheme of cutting samples is shown in Fig. 1. All samples were tested on a pendulum copra type IO-5003.

The hardness of the analyzed blade was measured by the ultrasonic method using the NOVOTEST portable universal rigidity tester.

The chemical composition of steel was determined on prismatic specimens 20×20×4 mm, using an atomic emission spectrometer SPECTROMAX LMF 0.5.

The metallographic features of the blade metal were studied using SEM EVO-40XVP with an INCA Energy 350 spectral microanalysis system.

Results of mechanical tests. The hardness was measured along the blade plate along the lines of inflection on the concave and convex surfaces of its plate parts and on the surface of the shank. It was established that the average values of 15Kh11MF steel hardness on the surfaces of the blade plate were 264 and 260 HB, and on the surface of the shank it was 260 HB (Table 2). On the basis of these measurements, it was found that the hardness of the 15Kh11MF steel along the length of the blade changed insignificantly, which indicates the uniformity of hardening and tempering of the blade during its heat treatment. However, according to current regulatory documents, the hardness of the steel blade should be within 241...244 HB. The obtained values of the hardness of the blade metal are higher than the set limit, which increases the tendency of the metal to brittle fracture.

Table 2

Hardness HB of the 15Kh11MF steel of the TPP rotor blade

Place of cutting	Blade surface	HB	HB^{av}
The profile part of the blade plate	concave	255...270	264
	convex	241…275	260
Shank part of the blade		245…272	260
Regulated hardness level		241…244	

The impact toughness is considered basic for determining the technical condition of the metal during routine inspections or maintenances. According to the results of impact tests of specimens from the profile part of the blade plate, the values of impact viscosity were KCU = 1.41 MJ/m^2, KCV = 0.99 MJ/m^2, and from its shank part KCV = 0.87 MJ/m^2 (Table 3). In accordance with the requirements of regulatory documents (GOST 5949-2018), KCV values of 15Kh11MF steel should not be lower than 0.39 MJ/m^2, and KCU values ≥ 0.59 MJ/m^2. Therefore, the obtained values of the impact toughness of the analyzed blade do not exceed the regulated levels. More than twice the impact toughness of a steel blade indicates that its resistance to brittle failure is high enough to minimize the possibility of its failure on impact. Therefore, it was believed that its fracture due to a one-time (even shock) overload is unlikely.

Table 3

Impact toughness of the 15Kh11MF steel of the TPP rotor blade

Place of specimen cut	KCU, MJ/m^2	KCV, MJ/m^2
The plate part of the blade	1.41	0.99
Shank part of the blade	–	0.87

The strength and plasticity characteristics of 15Kh11MF steel were analyzed on specimens from the peripheral (deformed) and from the blade plate located near its shank part and from the blade shank itself (Fig. 1). The strength and plasticity characteristics obtained from the results of the tensile tests of the specimens are given in Table. 4. Practical invariance of the strength characteristics along the plate of the peripheral part of the blade were observed. The average values of the ultimate tensile strength σ_{UTS} of steel, determined on all specimens, were 801 to 815 MPa, and the yield strength σ_{YS} were 710 and 690 MPa, respectively. These values do not exceed the requirements regulated for 15Kh11MF steel ($\sigma_{UTS} \geq 784$ MPa, σ_{YS} = (666...813) MPa after heat treatment in the quenching mode from 1050°C + tempering at 680°C), and also correspond to the values specified by supply certificate (σ_{UTS} = 785 and 809 MPa, σ_{YS}= 677 and 706 MPa). The characteristics of strength and plasticity of the shank part and near shank part of the blade were also within the regulated values (Table 4).

Table 4

Mechanical characteristics of the 15Kh11MF steel of the TPP rotor blade

Place of cutting	σ_{UTS}, MPa	σ_{YS}, MPa	δ, %	ψ, %	σ_{YS} / σ_{UTS}
Peripheral part of the blade plate	815	690	8.3	69.8	0.85
	801	710	7.4	64.5	0.89
Near shank part of the blade plate	786	630	11.5	63.0	0.80
Shank part of the blade	786	627	11.0	64.2	0.80
Regulated values, according to GOST 5949-2018					
15Kh11MF steel	≥ 690	≥ 490	≥ 15.0	≥ 55.0	-

The relative elongation δ of steel from all analyzed parts of the blade was lower than the regulated value, and the relative narrowing met the requirements for 15Kh11MF steel (Table 4). In the supply certificate, the values are also higher, namely δ = 17% and ψ = 57%. The relative elongation of the blade metal was from 7.4 to 11.5%, which turned out to be lower than the regulated level, and indicates a low margin of plasticity of the used steel. In addition, the ratio σ_{YS} / σ_{UTS}, which varied within 0.80...0.89, also confirms the low margin of plasticity of the blade metal.

Metallographic studies. The microstructure of the blade was studied on transverse sections from the peripheral part of the blade plate located at a distance of up to 50 mm from its fracture surface. The structure of the blade plate around its leading edge, which was surface hardened by electrospark alloying technology, the morphology of surface damage and the structure of the base metal of the blade plate were analyzed.

The macro heterogeneity of the surface hardened layer structure on the leading edge of the blade, obtained by the electrospark alloying method, porosity and uneven distribution of carbides of refractory elements in the cross-section were noted. The thickness of this layer varied and was a maximum of 160 μm near the leading edge of the blade and a minimum of 45 μm on separate sections of its convex surface (Fig. 2). Refractory tungsten carbides or intermetallic compounds (of the Fe_7W_6 type) in the hardened layer were located along the boundaries of columnar grains of ferrite highly alloyed with chromium, approaching the boundary with the base metal of the blade (Fig. 2 *a*). Their morphology is determined by the direction of heat removal during the cooling of molten metal microvolumes at the contact points of the electrodes during electrospark alloying with the cold surface of the blade plate. As the distance from the blade surface increased, the grains in the layer structure became rounded, and the spherical tungsten carbides became comparable in size to them (Fig. 2 *b*). At an even greater distance from the blade base metal, chromium carbides were released from the highly

chromium-alloyed matrix (Fig. 2 *c*). Their clusters formed star-shaped elements on the background of the alloyed matrix, and small tungsten carbides were found only occasionally along their boundaries. Bands with similar structural features alternated throughout the thickness of the layer.

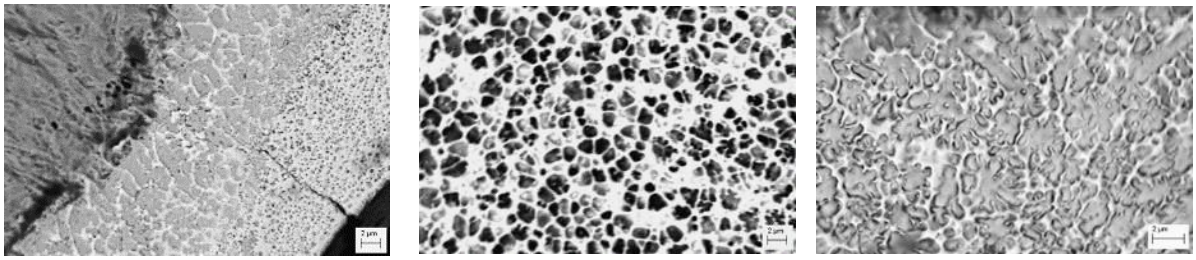

a *b* *c*

Figure 2. Microstructure of the surface hardened layer on the leading edge of blade

By X-ray microspectral analysis it was established (Fig. 3) that the main alloying elements of the surface hardened layer obtained by the electrospark alloying method were Ti, Co, Cr, W. In the surface hardened layer of the blade, the average content of elements was, wt. %: 1.8 Ti 2.2 Co, 10.1 Cr and 29.7 W. Moreover, the lighter the areas in the cover structure, the higher the content of W and Cr and the lower the content of Fe, and vice versa when the areas are darker. Bright white inclusions in the electrospark alloyed surface hardened layer had an increased content of Cr and Fe and were therefore considered to be tungsten carbides or intermetallics. Areas of light gray background corresponded to chromium doped ferrite.

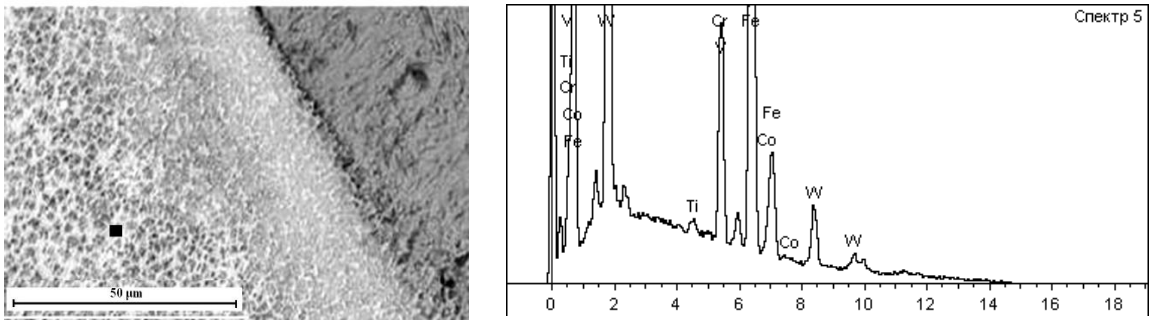

Figure 3. X-ray microspectral analysis of the blade surface hardened layer

A significant number of large round pores was noticed on the surface of the blade layer hardened by electrospark alloying technology. Their maximum size reached 30 µm (Fig. 4a). The growth of cracks was recorded from almost all observed pores, due to which gave it was possible to consider them as ready-made stress concentrators that facilitated the nucleation of fatigue cracks in the surface layer and, accordingly, their propagation into the blade body (Fig. 4b, c). Such technological defects of steam turbine blades were considered one of the main reasons for their premature destruction [28, 29]. These cracks were recorded on the transverse section. It is obvious that on the axial grind, due to the favorable tensile load scheme of the leading edge of the blade, it was possible to record a larger number of cracks (including those that would grow into the body of the blade). In particular, on the surface that corresponded to the fracture surface of one of these cracks, oriented across the blade plate and located slightly below the

surface of the cutting wheel (therefore not damaged during its manufacture), the characteristic signs of fatigue crack propagation, namely, small fatigue grooves could be seen. It was located at a distance of almost 5 mm from the leading edge on the side of the convex surface of the blade. Based on the analysis of defects in the surface layer of the blade, it was considered that the presence of large pores could cause its fatigue cracking during operation.

Figure 4. Cracks in the of the surface hardened layer of the blade

At the boundary of the surface-strengthened layer and the base of 15Kh11MF steel blade plate, a chain of pores up to 7 μm in size, caused either by the Kirkendall effect (due to unequal counter-diffusion of alloying elements across the boundary between the blade and the ESA layer), or by unsatisfactory preparation of the surface of the blade before use was observed.

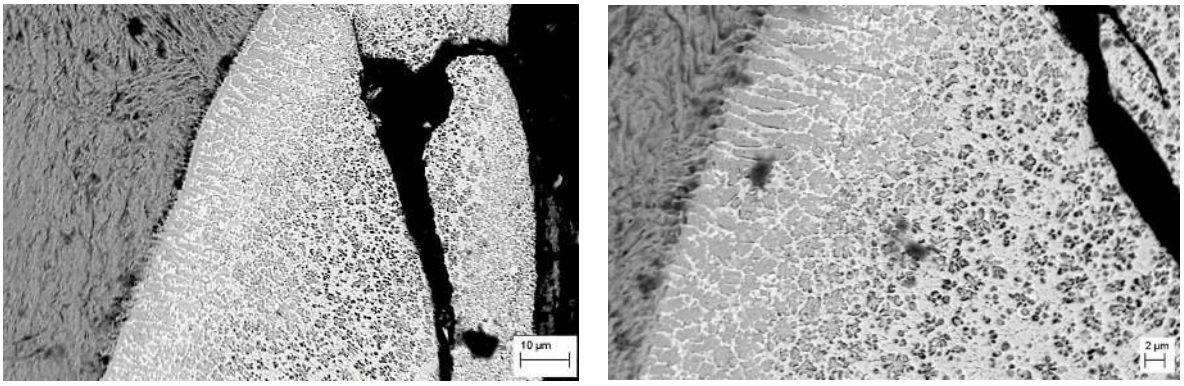

a b

Figure 5. Chains of pores at the boundary between the base metal and the surface hardened layer formed by electrospark alloyed method

Tensile stresses of up to 500 MPa can occur at the boundary, which, when combined with the working stresses acting on the blade, can significantly affect their fatigue life (especially under the influence of condensate with aggressive components dissolved in it) and, thereby, significantly reduce their service life. These chains facilitated the penetration of cracks from the electrospark alloyed layer into the base metal of the blade, and, therefore, contributed to the destruction of the blade.

A loosely structured layer of the base metal of the blade up to 10 μm thick was adjacent directly to the surface hardened layer using the electrospark alloying technology, within which the needle structure of sorbite (high-tempered martensite) was less clear than in the base metal of the blade. In general, the blade plate steel had a sorbite-like pearlite structure that inherited the martensite parallel crystal packet morphology characteristic of this type of hardened steel after high tempering. A fairly uniform distribution of crystal sizes in the blade was noted, which

is obviously due to the uniform distribution of former austenite grains by size, within which martensite crystals were formed (the average grain size was 52 μm) (Fig. 6 *a*).

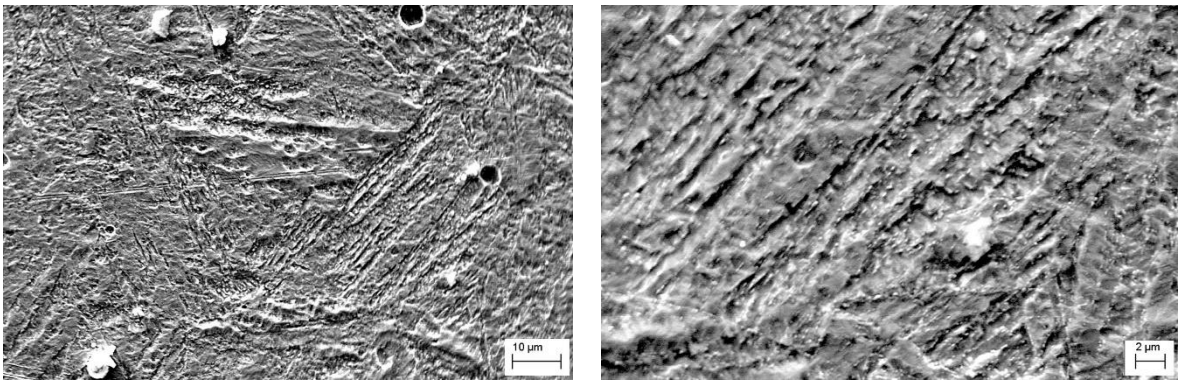

a *b*

Figure 6. Microstructure of the base metal of the of steam turbine rotor blade

At a high resolution in the structure of the blade plate, the allocation of very small carbides (0.05 μm) along the boundaries of the packets and unevenly distributed (not on all boundaries) slightly larger carbides along the boundaries of former austenite grains up to 0.8 μm in size were observed for complex chromium-based carbides (Fig. 6*b*). It is evident that the release of carbides along grain boundaries and packets of needle-like formations reduces the chromium content in the matrix. In addition, in the cross-section of the blades, a significant number of non-metallic 2...7 μm inclusions were found, around which cavities were formed, which is also an undesirable structural factor affecting the performance of such elements as steam turbine rotor blades.

Conclusions. After analyzing the mechanical properties of the 15Kh11MF steel of the steam turbine rotor blades, the most likely causes of its destruction were established. It is shown that in terms of mechanical properties during tensile and impact tests, the steel meets the requirements of the regulated documents. Non-compliance with these requirements was detected only by the relative elongation of steel, which as a rule is considered a sign of its low margin of plasticity.

Metallographic analysis revealed unsatisfactory melting of the surface of electrospark alloyed strengthened layer, which contributed to the appearance of large pores on its surface. This created extra stress concentration around the leading edge of the blade. In addition, the uneven thickness of the reinforced surface hardened layer and the low plasticity of the blade plate metal also contributed to the appearance of cracks in the blade under the action of working loads. A change in the frequency of natural oscillations of the blade (due to the cracking of its surface hardened layer) contributes for its resonance with a corresponding increase in the load amplitude. In the presence of an increased stresses concentration (pores and microcracks in the surface hardened layer of the blade) and the possibility of contact of the blade base metal with condensate (with aggressive components of the technological environment dissolved in it), favorable conditions have been created for corrosion-fatigue subcritical crack growth in the cross section of the blade plate up to its destruction.

References

1. Babii L. O., Student O. Z., Zagórski A. Markov A. D. Creep of degraded 2.25Cr-Mo steel in hydrogen. Materials Science. 2007. 46 (5). P. 701–707. https://doi.org/10.1007/s11003-008-9013-2
2. Marushchak P. O., Bishchak R. T., Gliha B, Sorochak A. P. Influence of temperature on the impact toughness and dynamic crack resistance of 25Kh1M1F steel. Materials Science 2011. 46 (4). P. 568–572. https://doi.org/10.1007/s11003-011-9325-5
3. Kurek M., Lagoda T., Walat K. Variations of Selected Cyclic Properties Depending on Testing Temperature. Materials Science. 2015. Vol. 50. P. 555–563. https://doi.org/10.1007/s11003-015-9753-8

4. Student O. Z., Matysiak H., Zagórski A., Babiy L. O., Kurzydlowski K. J. Creep rupture strength in hydrogen of Cr-Mo-V steel. Inżynieria powierzchni. 2005. 1 (2A). P. 175–179.
5. Zagórski A., Student O., Babij L., Nykyforchyn H., Kurzydłowski K. J. Peculiarities of hydrogen effect on the creep process in the Cr-Ni-Mo steel. Advances in Materials Science. 2007. Vol. 7, No. 1 (11). P. 211–218.
6. Dzioba I. R. Properties of 13KhMF steel after operation and degradation under the laboratory conditions. Materials Science. 2010. 46 (5). P. 357–354. https://doi.org/10.1007/s11003-010-9297-x
7. Student O. Z., Krechkovska H. V., Svirska L. M. Kindratskyi B. I., Shyrokov V. V. Ranking of the mechanical characteristics of steels of steam pipelines of thermal power plants by their sensitivity to in-service degradation. Materials Science. 2021. 57 (3). P. 404–412. https://doi.org/10.1007/s11003-021-00554-x
8. Marushchak P. O., Bishchak R. T., Gliha B., Sorochak A. P. Influence of temperature on the impact toughness and dynamic crack resistance of 25Kh1M1F steel. Materials Science. 2007. 46 (5). P. 568–552. https://doi.org/10.1007/s11003-011-9325-5
9. Romaniv O. M., Nykyforchyn H. M., Dzyuba I. R., Student O. Z., Lonyuk B. P. Effect of damage in service of 12Kh1MF steam-pipe steel on its crack resistance characteristics. Materials Science. 1998. 34 (1), P. 110–114. https://doi.org/10.1007/BF02362619
10. Krechkovs'ka H. V., Student O. Z. Determination of the degree of degradation of steels of steam pipelines according to their impact toughness on specimens with different geometries of notches. Materials Science. 2017. 52 (4). P. 566–571. https://doi.org/10.1007/s11003-017-9991-z
11. Miao X., Hong H., Hong X., Peng J., Bie F. Effect of Constraint and Crack Contact Closure on Fatigue Crack Mechanical Behavior of Specimen under Negative Loading Ratio by Finite Element Method. Metals – Open Access Metallurgy Journal. 2022. 12 (11). 1858. https://doi.org/10.3390/met12111858
12. Azeez A., Norman V., Eriksson R., Leidermark D., Moverare J. Out-of-phase thermomechanical fatigue crack propagation in a steam turbine steel – Modelling of crack closure. International Journal of Fatigue. 2021. Vol. 149. 106251. https://doi.org/10.1016/j.ijfatigue.2021.106251
13. Azeez A., Eriksson R., Leidermark D., Calmunger M. Low cycle fatigue life modelling using finite element strain range partitioning for a steam turbine rotor steel. Theoretical and Applied Fracture Mechanics. 2020. Vol. 107. 102510. https://doi.org/10.1016/j.tafmec.2020.102510
14. Maruschak P., Vorobel R., Student O., Ivasenko I., Krechkovska H., Berehulyak O., Mandziy T., Svirska L., Prentkovskis O. Estimation of fatigue crack growth rate in heat-resistant steel by processing of digital images of fracture surfaces. Metals. 2021. 11. 1776. https://doi.org/10.3390/met11111776
15. Nykyforchyn H. M., Tkachuk Yu. M., Student O. Z. In-service degradation of 20Kh13 steel for blades of steam turbines of thermal power plants. Materials Science. 2011. 47 (4). P. 447–456. https://doi.org/10.1007/s11003-012-9415-z
16. Ostash O. P., Panasyuk V. V., Andreiko I. M., Chepil R. V., Kulyk V. V., Vira V. V. Methods for the construction of the diagrams of fatigue crack-growth rate of materials. Materials Science. 2007. 43 (4). P. 479–491. https://doi.org/10.1007/s11003-007-0056-6
17. Rhode M., Nietzke J., Richter T., Mente T., Mayr P., Nitsche A. Hydrogen effect on mechanical properties and cracking of creep-resistant 9% Cr P92 steel and P91 weld metal. Welding in the World. 2023. 67. P. 183–194. https://doi.org/10.1007/s40194-022-01410-5
18. Toribio J., Vergara D. Lorenzo M. Role of in-service stress and strain fields on the hydrogen embrittlement of the pressure vessel constituent materials in a pressurized water reactor. Engineering Failure Analysis.2017. 82, P. 458–465. https://doi.org/10.1016/j.engfailanal.2017.08.004
19. Ostash O. P., Vytvyts'kyi V. I. Duality of the action of hydrogen on the mechanical behavior of steels and structural optimization of their hydrogen resistance. Materials Science. 2012. 47 (4). P. 421–737. https://doi.org/10.1007/s11003-012-9413-1
20. Sergeev N. N., Sergeev A. N., Kutepov S. N., Kolmakov A. G., Gvozdev A. E. Mechanism of the Hydrogen Cracking of Metals and Alloys, Part I (Review). Inorganic Materials: Applied Research. 2019. 10 (1). P. 24–31. https://doi.org/10.1134/S207511331901026X
21. Song Y., Chai M., Han Z., Liu P. High-Temperature Tensile and Creep Behavior in a CrMoV Steel and Weld Metal. Materials. 2022. 15 (1). 109. https://doi.org/10.3390/ma15010109
22. Yasniy O., Pyndus Y., Iasnii V., Lapusta Y. Residual lifetime assessment of thermal power plant superheater header. Engineering Failure Analysis. 2017. 82. P. 390–403. https://doi.org/10.1016/j.engfailanal.2017.07.028
23. Duriagina Z. A., Kulyk V. V., Filimonov O. S., Trostianchyn A. M., Sokulska N. B. The Role of Stress-Strain State of Gas Turbine Engine Metal Parts in Predicting Their Safe Life, Progress in Physics of Metals. 2021. 22 (4). P. 643–677. https://doi.org/10.15407/ufm.22.04.643
24. Smiyan O. D., Student O. Z. Fractographic signs of gigacycle fatigue and hydrogenation of heat-resistant steels after long-term operation. Material Science. 2021. 56 (6). P. 727–738. https://doi.org/10.1007/s11003-021-00489-3

25. Krechkovs'ka H. V., Student O. Z., Nykyforchyn H. M. Diagnostics of the engineering state of steam pipelines of thermal power plants by the hardness and crack resistance of steel. Materials Science. 2019. 54 (5). P. 627–637. https://doi.org/10.1007/s11003-019-00227-w
26. DSTU ISO 6892-1:2019 Metalevi materialy. Vyprobuvannia na roztiah. Chastyna 1. Metod vyprobuvannia za kimnatnoi temperatury (ISO 6892-1:2016, IDT).
27. DSTU ISO 148-1:2022 Metalevi materialy. Vyprobuvannia na udarnyi vyhyn za Sharpi na maiatnykovomu kopri. Chastyna 1. Metod vyprobuvannia (ISO 148-1:2016, IDT).
28. Krechkovska H., Hredil M., Student O., Svirska L., Krechkovska S., Tsybailo I., Solovei P. Peculiarities of fatigue fracture of high-alloyed heat-resistant steel after its operation in steam turbine rotor blades. International Journal of Fatigue. Vol. 167. Part B. 2023. 107341. https://doi.org/10.1016/j.ijfatigue.2022.107341
29. Krechkovska H., Hredil M., Student O. Book chapter 28: Fatigue crack growth resistance of heat-resistant steel 15H11MF after operation in blades of a steam turbine. Fatigue and Fracture of Materials and Structures / Eds. G. Lesiuk, S. Duda, J. A. F. O. Corea, A. M. P. De Jesus, Structural Integrity 24. Springer Nature Switzerland AG, 2022. P. 245-251. https://doi.org/10.1007/978-3-030-97822-8_28

Список використаних джерел

1. Babii L. O., Student O. Z., Zagórski A. Markov A. D. Creep of degraded 2.25Cr-Mo steel in hydrogen. Materials Science. 2007. 46 (5). P. 701–707. https://doi.org/10.1007/s11003-008-9013-2
2. Marushchak P. O., Bishchak R. T., Gliha B, Sorochak A. P. Influence of temperature on the impact toughness and dynamic crack resistance of 25Kh1M1F steel. Materials Science 2011. 46 (4). P. 568–572. https://doi.org/10.1007/s11003-011-9325-5
3. Kurek M., Lagoda T., Walat K. Variations of Selected Cyclic Properties Depending on Testing Temperature. Materials Science. 2015. Vol. 50. P. 555–563. https://doi.org/10.1007/s11003-015-9753-8
4. Student O. Z., Matysiak H., Zagórski A., Babiy L. O., Kurzydlowski K. J. Creep rupture strength in hydrogen of Cr-Mo-V steel. Inżynieria powierzchni. 2005. 1 (2A). P. 175–179.
5. Zagórski A., Student O., Babij L., Nykyforchyn H., Kurzydłowski K. J. Peculiarities of hydrogen effect on the creep process in the Cr-Ni-Mo steel. Advances in Materials Science. 2007. Vol. 7, No. 1 (11). P. 211–218.
6. Dzioba I. R. Properties of 13KhMF steel after operation and degradation under the laboratory conditions. Materials Science. 2010. 46 (5). P. 357–354. https://doi.org/10.1007/s11003-010-9297-x
7. Student O. Z., Krechkovska H. V., Svirska L. M. Kindratskyi B. I., Shyrokov V. V. Ranking of the mechanical characteristics of steels of steam pipelines of thermal power plants by their sensitivity to in-service degradation. Materials Science. 2021. 57 (3). P. 404–412. https://doi.org/10.1007/s11003-021-00554-x
8. Marushchak P. O., Bishchak R. T., Gliha B., Sorochak A. P. Influence of temperature on the impact toughness and dynamic crack resistance of 25Kh1M1F steel. Materials Science. 2007. 46 (5). P. 568–552. https://doi.org/10.1007/s11003-011-9325-5
9. Romaniv O. M., Nykyforchyn H. M., Dzyuba I. R., Student O. Z., Lonyuk B. P. Effect of damage in service of 12Kh1MF steam-pipe steel on its crack resistance characteristics. Materials Science. 1998. 34 (1), P. 110–114. https://doi.org/10.1007/BF02362619
10. Krechkovs'ka H. V., Student O. Z. Determination of the degree of degradation of steels of steam pipelines according to their impact toughness on specimens with different geometries of notches. Materials Science. 2017. 52 (4). P. 566–571. https://doi.org/10.1007/s11003-017-9991-z
11. Miao X., Hong H., Hong X., Peng J., Bie F. Effect of Constraint and Crack Contact Closure on Fatigue Crack Mechanical Behavior of Specimen under Negative Loading Ratio by Finite Element Method. Metals – Open Access Metallurgy Journal. 2022. 12 (11). 1858. https://doi.org/10.3390/met12111858
12. Azeez A., Norman V., Eriksson R., Leidermark D., Moverare J. Out-of-phase thermomechanical fatigue crack propagation in a steam turbine steel – Modelling of crack closure. International Journal of Fatigue. 2021. Vol. 149. 106251. https://doi.org/10.1016/j.ijfatigue.2021.106251
13. Azeez A., Eriksson R., Leidermark D., Calmunger M. Low cycle fatigue life modelling using finite element strain range partitioning for a steam turbine rotor steel. Theoretical and Applied Fracture Mechanics. 2020. Vol. 107. 102510. https://doi.org/10.1016/j.tafmec.2020.102510
14. Maruschak P., Vorobel R., Student O., Ivasenko I., Krechkovska H., Berehulyak O., Mandziy T., Svirska L., Prentkovskis O. Estimation of fatigue crack growth rate in heat-resistant steel by processing of digital images of fracture surfaces. Metals. 2021. 11. 1776. https://doi.org/10.3390/met11111776
15. Nykyforchyn H. M., Tkachuk Yu. M., Student O. Z. In-service degradation of 20Kh13 steel for blades of steam turbines of thermal power plants. Materials Science. 2011. 47 (4). P. 447–456. https://doi.org/10.1007/s11003-012-9415-z
16. Ostash O. P., Panasyuk V. V., Andreiko I. M., Chepil R. V., Kulyk V. V., Vira V. V. Methods for the construction of the diagrams of fatigue crack-growth rate of materials. Materials Science. 2007. 43 (4). P. 479–491. https://doi.org/10.1007/s11003-007-0056-6

свідчить про низький запас пластичності металу лопатки, що сприяло його розтріскуванню під дією робочих навантажень. Встановили, що середні значення твердості сталі 15Х11МФ на поверхнях пера лопатки становили 264 та 260 НВ, а на поверхні хвостовика – 260 НВ. На основі цих замірів констатували, що твердість сталі 15Х11МФ по довжині лопатки змінювалася неістотно, що свідчить про рівномірність прогартовування й відпуску лопатки під час її термічного оброблення. Металографічним аналізом встановили, що сталь 15Х11МФ пера лопатки має структуру сорбіт-подібного перліту, який спадкував морфологію пакетів з паралельних кристалів мартенситу, що властиво такого типу гартованим сталям після високого відпуску. Відзначили достатньо рівномірний розподіл за розмірами кристалів у лопатці, що, очевидно, зумовлено рівномірним розподілом колишніх зерен аустеніту за розмірами, в межах яких формувалися кристали мартенситу (середній розмір зерна становив 52 мкм). Відзначили макронеоднорідність структури поверхнево-зміцненого шару на вхідній крайці лопатки, отриманого методом ЕІЛ, пористість та нерівномірність розподілу карбідів тугоплавких елементів у поперечному перерізі. В околі основного металу лопатки тугоплавкі карбіди вольфраму або інтерметаліди (типу Fe_7W_6) розташовувалися у вигляді оторочки вздовж меж стовпчастих високолегованих хромом феритних зерен. Виявлено пори в поверхнево-зміцненому шарі лопатки, які спричинили низьку адгезію шару з основним металом лопатки, а також стали осередками зародження тріщин. Висока концентрація напружень (пори і мікротріщини в поверхнево-зміцненому шарі лопатки) та контакт металу лопатки з робочим середовищем, сприяли корозійно-втомному докритичному росту тріщини у поперечному перерізі її пера аж до наскрізного руйнування.

Ключові слова: *сталі 15Х11МФ, лопатка парової турбіни, міцність, пластичність, ударна в'язкість, структура.*

https://doi.org/10.33108/visnyk_tntu2023.02.046 *Отримано 02.03.2023*